NANO LETTERS

Letter

pubs.acs.org/NanoLett

Guided Growth of Epitaxially Coherent GaN Nanowires on SiC

David Tsivion and Ernesto Joselevich*

Department of Materials and Interfaces, Weizmann Institute of Science, Rehovot 76100, Israel

Supporting Information

ABSTRACT: We report the guided growth of highly coherent, horizontal GaN nanowires (NWs) on atomically flat singular SiC (0001) and on periodically stepped vicinal SiC (0001) substrates. On singular SiC (0001) the NWs grow in six symmetry-equivalent directions, while on vicinal SiC (0001) the NWs grow only in the two directions parallel to the atomic step edges. All of the NWs have the same epitaxial relations with the substrate on both singular and vicinal (0001). Owing to the low mismatch (~3.4%) with the substrate, the NWs grow highly coherent, with a much lower density of misfit dislocations than previously observed on sapphire. This is also the first observation of NW VLS growth along atomic steps. Epitaxially coherent guided NWs have potential uses in many fields, including high-power electronics, light-emitting diodes (LEDs), and laser diodes.

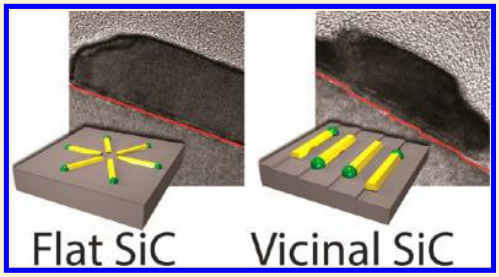

KEYWORDS: *Nanowires, gallium nitride, silicon carbide, epitaxy, self-assembly, bottom-up*

Semiconductor nanowires (NWs) are promising building blocks for a wide variety of nanodevices.[1] A vast variety of NW-based devices have been demonstrated, including field-effect transistors,[2,3] lasers,[4,5] light-emitting diodes,[6,7] photovoltaic cells,[8−10] chemical and biological sensors,[11−13] and piezoelectric nanogenerators.[14] A promising route to the bottom-up synthesis of nanodevices is the vapor−liquid−solid (VLS) growth, where a nanometric metal droplet (the catalyst) collects precursor species form the gas phase and, upon reaching supersaturation, deposits a NW.[15] The NWs grown by this method usually grow vertically off the surface of a substrate, while the growth directions can be controlled by the epitaxial relations with the substrate. These NWs have excellent properties[16] since they are nanometric in size and grow stress-free and as a result contain few strain-related defects. While this VLS approach produces high-quality NWs, there still remains a problem toward large-scale integration into functional systems. To organize the NWs on surfaces, most common approaches start by harvesting the NWs, dispersing them in solution, and then controlling their deposition on a surface.[17] These postgrowth approaches suffer from thermal and dynamic fluctuations, and consequently, the alignment is not perfect. Furthermore, the harvesting step often damages these thin NWs and contaminates them with solvent residues.

In contrast to these postgrowth assembly methods, in the guided growth approach the NWs are assembled and organized during the growth process. The NWs also grow from a catalyst, but here the metal droplet maintains contact with the substrate while "crawling" on the surface. Following the catalyst droplets, the NWs grow horizontally on the surface of the substrate, guided as they grow either epitaxially by the interaction with the substrate lattice, or by graphoepitaxy, that is, the interaction with surface features such as nanogrooves or nanosteps.[18,19] This approach can produce NWs with controlled orientations, lengths, geometry, and even precise location,[20] and therefore this approach is a promising route for realizing the vision of bottom-up nanofabrication.

The guided growth of NWs has so far been demonstrated for GaAs NWs on GaAs (100)[21] (homoepitaxial growth) and for ZnO NWs on sapphire[19,22] and on GaN[23] and for GaN NWs on sapphire[18] (heteroepitaxial growth). When grown heteroepitaxially, there is lattice mismatch between the horizontal NWs and the substrate. This case can be further divided to coincident epitaxy (where an integer number of NW lattice planes matches perfectly with an integer number of substrate planes, and therefore both are completely relaxed) or incommensurate epitaxy (where a perfect matching of any integer number of NW/substrate planes is unavailable, and therefore there is residual strain in the NW and the substrate). In both cases, misfit dislocations appear at the NW/substrate interface. These dislocations relieve the interface strain partially or completely and do not evolve into threading dislocations in the NWs. However, the presence of misfit dislocations at semiconductor interfaces often has detrimental effects in applications such as high electron mobility transistors (HEMTs), where these defects can act as scattering centers, thereby lowering the carrier velocity.[24] To reduce the number of misfit dislocations, a substrate with closer crystallographic matching is needed. For example in the case of GaN, SiC is superior to sapphire because the basal plane of SiC has a lattice constant (a = 3.08 Å) very close to that of GaN (a = 3.19 Å), and hence the mismatch between them is only 3.4%. For comparison, the mismatch for GaN on the basal plane of sapphire, a common epitaxial substrate for GaN, is 16% (a = 4.78 Å).

Received: August 16, 2013
Revised: October 1, 2013
Published: October 17, 2013

Here we demonstrate the guided growth of horizontal GaN NWs on both singular (i.e., perfectly cut along a low-index crystallographic plane) and vicinal (i.e., cut with a slight tilt with respect to a low-index crystallographic plane) SiC substrates (Figure 1). The GaN NWs grown on flat (0001) SiC substrates

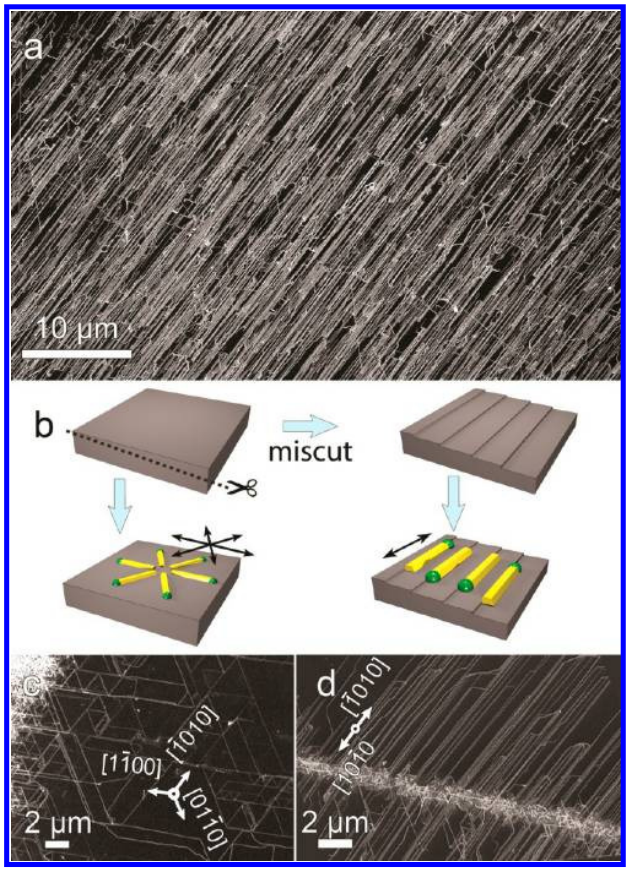

Figure 1. Guided growth of horizontal GaN NWs on SiC. (a) Highly dense, nonpatterned growth of GaN NWs on vicinal (0001) plane of 4H-SiC tilted by 4° toward [11$\bar{2}$0]. (b) Graphoepitaxial effect on the guided growth of horizontal ZnO NWs on (0001) SiC. (c) Triangular network of GaN NWs grown on the (0001) plane of SiC from patterned catalyst islands. The catalyst island edge is on the top left. (d) Patterned growth of GaN NWs from a catalyst island on vicinal (0001) plane of 4H-SiC tilted by 4° toward [11$\bar{2}$0]. The catalyst island is the white near-horizontal line.

are guided by lattice planes, resulting in a triangular network of NWs (Figure 1c), while the NWs grown on vicinal SiC substrates grow only in two directions parallel to the surface atomic steps (Figure 1a,d). We characterized the orientations, epitaxial relations, strain, and defects by high-resolution transmission electron microscopy (HRTEM). We found that the crystallographic orientation of all of the NWs is identical with respect to the (0001) SiC plane. Furthermore, we have found that, thanks to the low mismatch with the SiC substrate, the GaN NWs grow highly coherent, with a low density of misfit dislocation. Finally, we characterized the photoluminescence (PL) of the guided NWs and compare it with that of vertically grown NWs.

Results and Discussion. We grew guided GaN NWs on the Si-terminated face of three different SiC substrates: a (0001) plane of 6H-SiC and 4H-SiC, and a vicinal (0001) plane of 4H-SiC tilted by 4° toward [11$\bar{2}$0]. The growth was carried out by the vapor−liquid−solid (VLS) method in a three-zone furnace with a quartz tube reactor (see methods in the Supporting Information). The entire furnace was placed on a moving platform so that it could be preheated to the desired temperature without heating the substrate or the source material. Once the temperature is achieved, the furnace is moved to the desired location over the sample and the Ga precursor. The Ga and N elements were supplied from Ga_2O_3 powder and high-purity NH_3 gas. H_2 was used as a carrier gas. The Ga_2O_3 powder was held at a temperature of 1000 or 950 °C, while the sample was held at a temperature of 950 °C. The catalyst used for the VLS growth was Pd. Pd particles were either created by electron-beam evaporation of a thin (nominally 0.2−0.6 nm) layer, followed by dewetting at elevated temperature, or by drop-casting a solution of bis(dibenzylideneacetone) palladium in 1,2-dichloroethane. After the synthesis, the pattern was covered with a dense forest of GaN NWs growing vertically off the surface of the substrate. In addition, a large number of NWs grew horizontally from the pattern edges, extending onto the clean SiC surface. Brief sonication in isopropyl alcohol removes most of the NW forests, leaving the horizontal NWs in place. The typical NW thickness, d (defined here as their top-projection width), was between 5 and 50 nm. The NW lengths could be up to 60 μm. The height and width d of the NWs was found to correlate with the size of the catalyst droplet. However, toward the base of the NW, the width d slightly increased during the synthesis, presumably due to direct addition of material from the vapor phase to the NW sidewalls. The crystallographic structure, orientation, and epitaxial relations of the NW on the substrate were determined by cutting thin (50−100 nm) slices across the NWs using a focused ion beam (FIB) and observing them under HRTEM. Geometric phase analysis[25] of the TEM images was obtained using the GPA plug-in for DigitalMicrograph.

Guided GaN NWs grown on the (0001) plane of 4H-SiC and 6H-SiC were initially characterized using a scanning electron microscope (SEM). We have found the NWs extending from the edges of the catalyst pattern in six directions, creating of a triangular NW network (Figure 1c). We determined the epitaxial relations of the NWs and the substrate by examining cross-sectional lamellae using a TEM (Figure 2a−c). The planar epitaxial relations are $(0001)_{GaN} \parallel (0001)_{SiC}$, with $[10\bar{1}0]_{GaN} \parallel [10\bar{1}0]_{SiC}$ along the NW and $[11\bar{2}0]_{GaN} \parallel [11\bar{2}0]_{SiC}$ across the NW. This epitaxial relation is identical to the one reported in literature for thin films of GaN on SiC (0001). This epitaxial relation results in the triangular geometry of the NWs on the substrate, which is consistent with to the C_6 morphological symmetry of the (0001) SiC substrate. Both 6H-SiC and 4H-SiC can be described as hexagonal planes stacked along the [0001] direction, with a different stacking order. Therefore, an ideally flat (0001) plane of both 6H-and 4H-SiC has C_6 morphological symmetry with minute differences in the planar lattice parameter between the two polytypes (4H-SiC: a = 3.0730, 6H-SiC: a = 3.0806).

We also grew GaN NWs on vicinal (0001) 4H-SiC tilted by 4° toward [11$\bar{2}$0]. We have found that, on these substrates, the guided GaN NWs grow only in two directions, parallel to the step edges (Figures 1a,d and 3a−d). The NWs grow along the $[10\bar{1}0]_{SiC}$ direction which is parallel to the atomic steps. The epitaxial relation on these vicinal substrates turns out to be identical to that of GaN NWs grown on flat (0001) SiC. The surface of these vicinal substrates is not atomically flat like that

dx.doi.org/10.1021/nl4030769 | Nano Lett. 2013, 13, 5491−5496

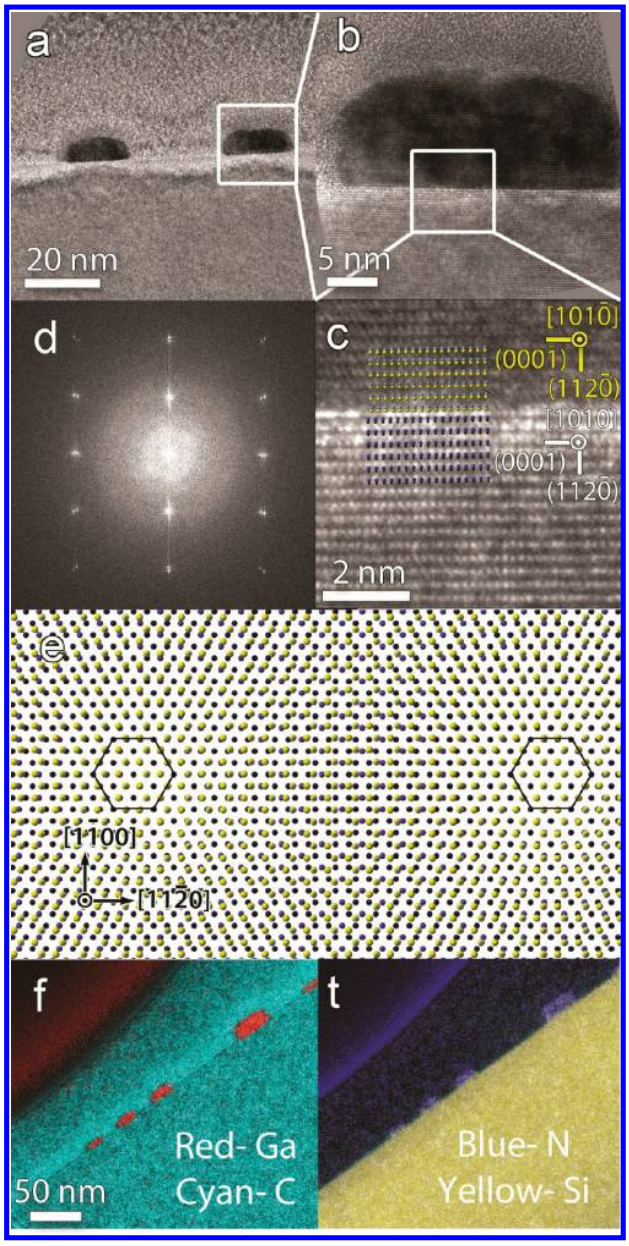

Figure 2. TEM cross-sectional images and atomic models of GaN NWs on flat (0001) SiC substrates. (a–c) Cross sections of GaN NWs on SiC substrates. White boxes indicate magnified areas. Image c includes the crystallographic orientations and proposed atomic models. (d) FFT of a cross-sectional TEM image. The image clearly shows two sets of closely matched diffraction spots, for the GaN and SiC. (e) Suggested atomic model for the atomic arrangement on the (0001) surface. (f,g) EELS elemental map of GaN on SiC (left: Ga and C, right: N and Si). No interdiffusion between NW and substrate is observed.

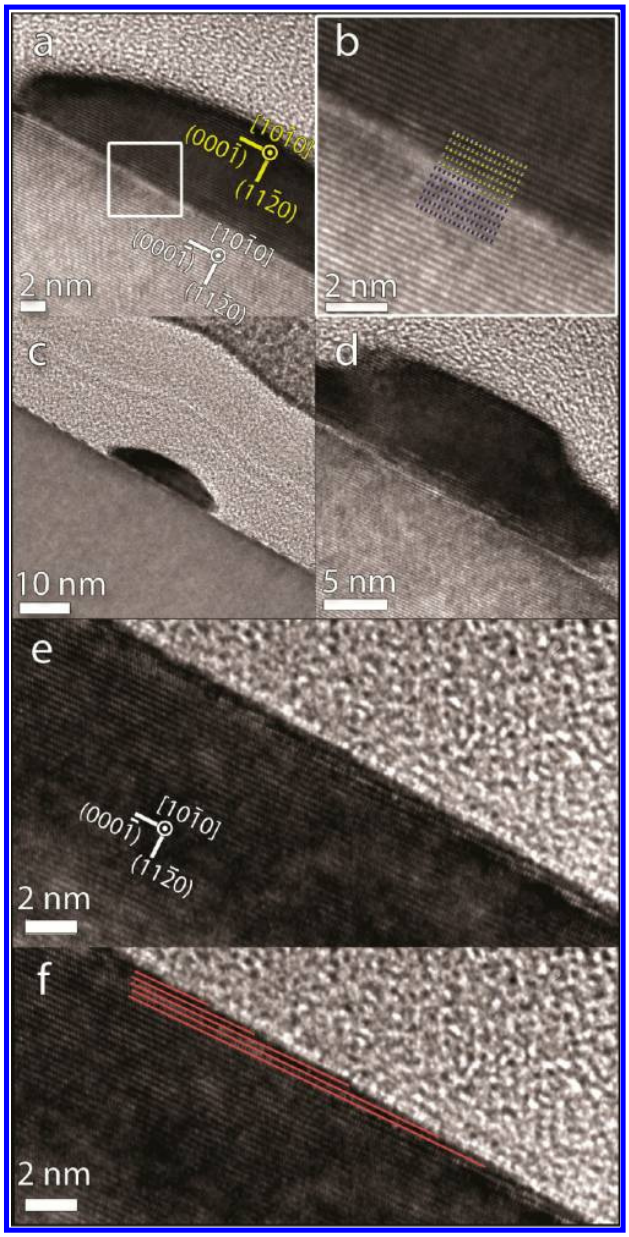

Figure 3. TEM cross-sectional images and atomic models of GaN NWs on vicinal (0001) plane of 4H-SiC tilted by 4° toward [11$\bar{2}$0]. (a–d) Cross sections of three GaN NWs on SiC substrates. Several atomic steps at the GaN/SiC interface are clearly seen in d. White boxes indicate magnified areas. Image b includes the proposed atomic models, including the atomic step. (e) TEM cross-sectional image of a clean vicinal substrate with atomic steps. (f) The same image as e with red lines highlighting the Si–C bilayers. All of the steps highlighted in this image are a single Si–C bilayer, 0.25 nm in height, and a quarter of a 4H-SiC unit cell.

of perfectly cut (0001) substrates but terminated with periodic atomic steps, which break the C_6 symmetry of the SiC (0001) plane. Most of these atomic steps characterized by TEM were found to be of one Si–C bilayer, 0.25 nm (Figure 3e,f). We speculate that these atomic steps interact with both the catalyst droplet and the growing NW, and as a result the NWs grow almost exclusively parallel to these atomic ledges (Figure 1b). A similar effect was previously reported only for higher steps created by bunching of atomic steps at elevated temperatures and for large (2–5 nm) nanogrooves formed by the high-temperature annealing of thermodynamically unstable crystal faces.[18,19] When the guiding relief features of the substrate is larger than the lattice parameter, it is usually referred to as graphoepitaxy,[26−28] whereas the guiding by steps lower than the lattice parameter is called ledge-directed epitaxy.[29,30]

dx.doi.org/10.1021/nl4030769 | *Nano Lett.* 2013, 13, 5491–5496

There are several differences between the graphoepitaxy reported previously for guided NW of GaN[18] and ZnO[19] on sapphire and the ledge-directed epitaxy reported here: (a) In the previous cases, a guiding effect was not pronounced when the synthesis was performed on the nonannealed vicinal sapphire (0001) substrate. The atomic steps on the nonannealed surface did not have a strong guiding effect on the NWs. Significant guiding was only observed after annealing the substrate at high temperature, which resulted in bunching of the 0.22 nm high sapphire atomic steps to larger steps of 2−4 nm height. In the case of GaN on SiC, no annealing step was needed to achieve a strong guiding effect. Interestingly, single-walled carbon nanotubes with a diameter of 0.8−3 nm were shown to grow along atomic steps on nonannealed vicinal sapphire substrates,[31] and the guiding effect along atomic steps was actually stronger than along bunched nanosteps. (b) When GaN was grown on sapphire, the graphoepitaxial effect caused the NWs to grow with crystallographic orientations that were different from the crystallographic orientations on the nearest singular substrate, which is atomically flat. Moreover, the graphoepitaxial effect caused variability in the crystallographic orientation of the NWs. This was attributed to the competing interaction of the NW and the catalyst droplet with two planes: the plane of the terrace and the plane of the step, or the two facets of a nanogroove. In contrast, the growth of GaN on vicinal SiC occurs in exactly the same crystallographic orientation and epitaxial relations as the growth on flat SiC substrate. The reason could be that the steps are in just the right size: large enough to influence the catalyst droplet and determine the growth direction, but not large enough to compete with the terrace over dictating the crystallographic orientation of the NW. It is interesting to note that one NW is wide enough to grow on several parallel steps simultaneously, as seen in Figure 3d. Although further research is needed to elucidate the specific mechanism that enforces the actual guiding along these surface steps, we can suggest two possible effects: (i) The catalyst droplet is pinned to the step due to preferential wetting. (ii) The interaction of the NW with the step edges is stronger than with the atomically flat surface due to the higher surface energy of the step edges, especially when the NW crystal lattice is aligned parallel to the atomic steps.

We further investigated the crystallographic structure, orientation, and elemental composition of the NWs by observing thin FIB-made cross-sectional lamellae using a HRTEM (Figure 2a−c). In general, the TEM images reveal lattice fringes expected of GaN and SiC. Elementary mapping of Ga, N, Si, and C by electron energy loss spectroscopy (EELS) reveals sharp GaN/SiC interfaces without observable interdiffusion (Figure 2f,g). A fast Fourier transformed image shows a double set of close peaks, for the GaN and the SiC substrate (Figure 2d). We superimposed proposed atomic models on the TEM image to highlight the structure and epitaxy (Figure 2c) and show a proposed atomic model of the planar epitaxial relations in top view (Figure 2e).

To characterize the nature of the NW/substrate interface, we measured the average lattice spacing in the NWs and the substrate, analyzed TEM images by Fourier filtering to reveal the presence of misfit dislocations, and used geometric phase analysis (GPA) to characterize the strain in the NWs near and away from the interface. Figure 4a (left) shows a TEM image of a NW cross-section. On the right, we show a Fourier-filtered part of the NW-substrate interface, with arrows indicating the two misfit dislocations present at the interface. The distance

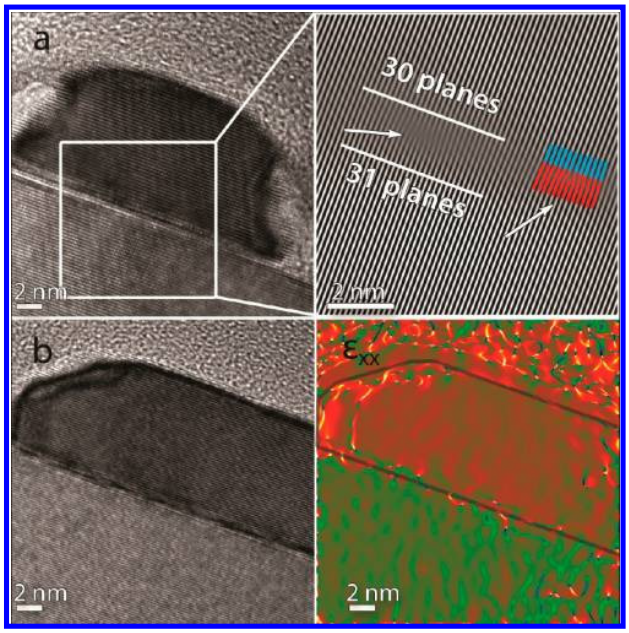

Figure 4. Mismatch, strain, and misfit dislocations in guided GaN NW on SiC. (a) A cross-sectional TEM image (left) with a Fourier-filtered FFT of the area indicated with a white box. Two misfit dislocations are indicated with arrows and highlighted with color. The 30 GaN planes match 31 SiC planes. (b) Left: Cross-sectional TEM image of GaN on vicinal SiC. Right: GPA image of the TEM image on the left, showing the in-plane strain ε_{xx}. The area of the NW is highlighted with a gray frame. The strain is uniform in the NW, indicating a relaxed NW with no residual strain.

between the misfit dislocations is exactly 31 SiC planes and 30 GaN planes. This spacing is exactly the spacing that we would expect form a naïve calculation of the optimal matching between the $[11\bar{2}0]$ planes of SiC and GaN: 1.54 Å × 31 ≈ 1.59 Å × 30. Any addition or subtraction of planes in the NW or in the substrate would result in a larger mismatch. To complement this observation, we measured the average values of lattice spacing and found that the average ratio of GaN $[11\bar{2}0]$ planes to SiC $[11\bar{2}0]$ planes is 1.0303 ± 0.004, very close to the bulk ratio of 1.034. Together, these observations indicate that there is only a very slight or no compression of the NW lattice, and therefore there is no further reduction in the density of misfit dislocation at the NW/substrate interface. Therefore, we conclude that the NW and the substrate are fully or almost fully relaxed. To further test this hypothesis, we used geometric phase analysis[25] to observe the variability of the in-plane lattice strain in the NWs (Figure 4b, right and left). As can be seen in the right part of Figure 3b (mapping of in-plane lattice strain, ε_{xx}), the strain is uniform in the NW, further strengthening our observation of a fully relaxed NW.

The significance of these findings can be understood in light of heteroepitaxial growth theory. When a layer is grown on a heterosubstrate, the total strain energy grows as the layer height increases. At a certain critical height h_c, the introduction of misfit dislocations at the interface becomes energetically favorable. These dislocations relieve some of the strain but have an energetic cost. The critical thickness h_c can be calculated for 2D films using eq 1, where b is the length of the Burgers vector, λ is the angle between the Burgers vector and the direction in the interface, ν is the Poisson ratio, and f is a mismatch between the substrate and the epilayer.[32] Using this

dx.doi.org/10.1021/nl4030769 | Nano Lett. 2013, 13, 5491−5496

equation, we calculated h_c = ~1.8 nm. In the case of NWs or nanoislands, this critical thickness increases due to increased ability of one or zero-dimensional structures to accommodate the strain.[33] However, we do not know what the increase in the critical thickness is for horizontal NWs. The minimal thickness of NWs we observed in this work was ~5 nm, and these NWs did have misfit dislocations. Consequently, this sets an upper limit on the critical thickness of the GaN-SiC system. To conclude this part, guided NWs are expected to have a larger critical thickness than their 2D counterparts, but the NWs observed here, with height down to 5 nm, are nonetheless above this critical height. Therefore, misfit dislocations do appear, albeit at very low density.

$$h_c = \frac{b\cos\lambda}{2f}\left\{1 + \left[\frac{(1 - \nu/4)}{4\pi(1+\nu)\cos^2\lambda}\right]\right\}\left(\ln\frac{h_c}{b}\right) \quad (1)$$

To further investigate the properties of these highly coherent, guided GaN NWs, we measured the photoluminescence (PL) spectra of the NWs (Figure 5). Using a confocal microscope

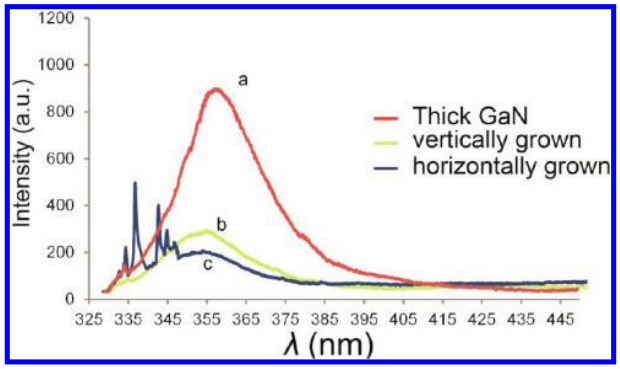

Figure 5. Optical properties of guided GaN NWs. Typical PL spectra at room temperature of (a) coalesced GaN growth at catalyst islands. (b) Vertically grown GaN NWs on (0001) SiC, dispersed on a sapphire substrate. (c) Horizontally grown GaN NWs on (0001) SiC. PL peak is blue-shifted ~3 nm with respect to the thicker GaN growth, on the same substrate, at the same synthesis. The sharp peaks on the left are Raman scattering from the sample.

with a He−Cd laser (325 nm), we measured the PL spectra of guided NWs and compared it with vertical GaN NWs as well as thicker GaN structures. In all of these cases, the PL spectra were typical of high-quality GaN with a single PL peak in the range of 328−740 nm. We did not see any yellow luminescence emission at 2.2 eV, a typical defect-induced emission in GaN. In general, the PL spectra we observed was very similar for (a) the thick, coalesed GaN growth found at the catalyst islands (Figure 5a), (b) vertical NWs that were dispersed on a sapphire substrate to avoid the PL of the SiC (Figure 5b), and (c) horizontally grown NWs (Figure 5c), all with λ_{max} between 354 and 357 nm. Interestingly, for thick GaN growth at the catalyst deposition area λ_{max} was at 357 nm, while for thin NWs, λ_{max} was 354 nm (for both vertically grown NWs and guided NWs). Possible reasons for this blue shift of thin NWs could be the emission from surface trap states, previously reported for GaN NWs in different crystallographic orientations,[34] and the high dielectric constant of the substrate. Strain could also lead to blue shift, but our analysis showed low strain, so that this effect is not expected to be dominant. Overall, we found the PL spectra of horizontally grown guided NWs to be very similar to those of vertical NWs, indicating that the interaction with the substrate does not induce defects that degrade the optical properties of the guided GaN NWs.

The mechanism behind the guided growth phenomenon is not yet fully understood. For example, previous reports on the guided growth of NWs claim that the reason that NWs grow in specific lattice directions is the anisotropic lattice mismatch.[35] However, in our case, this cannot explain the fact that the NWs grow in a specific direction, since the calculated lattice mismatch (3.4%) is isotropic on the flat SiC (0001) surface. Therefore, the explanation for the growth of NWs in a specific direction is not directly related to the lattice mismatch. We speculate that this preferred growth direction may be related to one or more of the following possible effects: (a) Minimization of the energy of the crystal facets of the NWs: the NW grows in the direction that produces the smallest overall facet energy. (b) The kinetics of crystal plane formation. In this case, the NW growth is determined by the kinetics of the growth process. It is worth mentioning that we did encounter some GaN NWs growing in the $[11\bar{2}0]$ direction, but these were a minority. However, the appearance of these NWs may indicate that the driving force toward growth in the $[10\bar{1}0]$ direction is not much stronger than the driving force for growth in the $[11\bar{2}0]$ direction, and as a result it may be possible to achieve growth in the $[11\bar{2}0]$direction by careful tuning of the synthetic parameters.

In summary, we have demonstrated the guided growth of horizontal GaN NWs on singular and vicinal SiC (0001) substrates. The use of these substrates enabled us to control the geometry of the NWs on the surfaces, changing from a triangular, 6-fold symmetry on flat (0001) SiC to 2-fold, linear geometry on stepped surfaces, while having identical epitaxial relations in both cases. These NWs were shown to be of high crystallographic perfection, growing stress-free and highly coherent, that is, with a low density of misfit dislocations at the substrate−NW interface. This work demonstrates the generality of the guided growth approach for a variety of substrates. The successful growth of GaN on SiC presented here, together with our previous work on GaN and ZnO on sapphire, shows that the guided growth approach, and its use in self-integrated nanosystems,[20] could be extended to a large variety of semiconductors and substrates. Since we are able to control the geometry and locations of these NWs on the surface, guided growth could enable the integration of NWs into a variety of nanodevices not available by other means, including high-power transistors, LEDs, and lasers.

■ ASSOCIATED CONTENT

Supporting Information

A detailed description of the materials and methods, SEM and image of the Pd catalyst prior to the NW growth (Figure S1), and additional SEM images of NW (Figures S2−S3). This material is available free of charge via the Internet at http://pubs.acs.org.

■ AUTHOR INFORMATION

Corresponding Author

*E-mail: ernesto.joselevich@weizmann.ac.il.

Notes

The authors declare no competing financial interest.

■ ACKNOWLEDGMENTS

We thank Dr. L. Zeiri for assistance with PL measurements. This research was supported by the Israel Science Foundation, Minerva Stiftung, Kimmel Center for Nanoscale Science, Moskowitz Center for Nano and Bio-Nano Imaging, and the Carolito Stiftung. D.T. acknowledges support from the Adams Fellowship Program of the Israel Academy of Science.

■ REFERENCES

(1) Lu, W.; Lieber, C. M. Nanoelectronics from the Bottom Up. *Nat. Mater.* **2007**, *6*, 841−850.
(2) Cui, Y.; Lieber, C. M. Functional Nanoscale Electronic Devices Assembled Using Silicon Nanowire Building Blocks. *Science* **2001**, *291*, 851−853.
(3) Huang, Y.; Duan, X. F.; Cui, Y.; Lauhon, L. J.; Kim, K. H.; Lieber, C. M. Logic Gates and Computation from Assembled Nanowire Building Blocks. *Science* **2001**, *294*, 1313−1317.
(4) Duan, X. F.; Huang, Y.; Agarwal, R.; Lieber, C. M. Single-Nanowire Electrically Driven Lasers. *Nature* **2003**, *421*, 241−245.
(5) Huang, M. H.; Mao, S.; Feick, H.; Yan, H. Q.; Wu, Y. Y.; Kind, H.; Weber, E.; Russo, R.; Yang, P. D. Room-Temperature Ultraviolet Nanowire Nanolasers. *Science* **2001**, *292*, 1897−1899.
(6) Gudiksen, M. S.; Lauhon, L. J.; Wang, J.; Smith, D. C.; Lieber, C. M. Growth of Nanowire Superlattice Structures for Nanoscale Photonics and Electronics. *Nature* **2002**, *415*, 617−620.
(7) Huang, Y.; Duan, X. F.; Cui, Y.; Lieber, C. M. Gallium Nitride Nanowire Nanodevices. *Nano Lett.* **2002**, *2*, 101−104.
(8) Law, M.; Greene, L. E.; Johnson, J. C.; Saykally, R.; Yang, P. D. Nanowire Dye-Sensitized Solar Cells. *Nat. Mater.* **2005**, *4*, 455−459.
(9) Tian, B.; Zheng, X.; Kempa, T. J.; Fang, Y.; Yu, N.; Yu, G.; Huang, J.; Lieber, C. M. Coaxial Silicon Nanowires as Solar Cells and Nanoelectronic Power Sources. *Nature* **2007**, *449*, 885−889.
(10) Yan, R. X.; Gargas, D.; Yang, P. D. Nanowire Photonics. *Nat. Photonics* **2009**, *3*, 569−576.
(11) Cui, Y.; Wei, Q. Q.; Park, H. K.; Lieber, C. M. Nanowire Nanosensors for Highly Sensitive and Selective Detection of Biological and Chemical Species. *Science* **2001**, *293*, 1289−1292.
(12) Kolmakov, A.; Zhang, Y. X.; Cheng, G. S.; Moskovits, M. Detection of Co and O-2 Using Tin Oxide Nanowire Sensors. *Adv. Mater.* **2003**, *15*, 997−1000.
(13) Wan, Q.; Li, Q. H.; Chen, Y. J.; Wang, T. H.; He, X. L.; Li, J. P.; Lin, C. L. Fabrication and Ethanol Sensing Characteristics of ZnO Nanowire Gas Sensors. *Appl. Phys. Lett.* **2004**, *84*, 3654−3656.
(14) Wang, Z. L.; Song, J. H. Piezoelectric Nanogenerators Based on Zinc Oxide Nanowire Arrays. *Science* **2006**, *312*, 242−246.
(15) Wagner, R. S.; Ellis, W. C. Vapor-Liquid-Solid Mechanism of Single Crystal Growth. *Appl. Phys. Lett.* **1964**, *4*, 89−90.
(16) Hu, J.; Odom, T. W.; Lieber, C. M. Chemistry and Physics in One Dimension: Synthesis and Properties of Nanowires and Nanotubes. *Acc. Chem. Res.* **1999**, *32*, 435−446.
(17) Wang, M. C. P.; Gates, B. D. Directed Assembly of Nanowires. *Mater. Today* **2009**, *12*, 34−43.
(18) Tsivion, D.; Schvartzman, M.; Popovitz-Biro, R.; von Huth, P.; Joselevich, E. Guided Growth of Millimeter-Long Horizontal Nanowires with Controlled Orientations. *Science* **2011**, *333*, 1003−1007.
(19) Tsivion, D.; Schvartzman, M.; Popovitz-Biro, R.; Joselevich, E. Guided Growth of Horizontal ZnO Nanowires with Controlled Orientations on Flat and Faceted Sapphire Surfaces. *ACS Nano* **2012**, *6*, 6433−6445.
(20) Schvartzman, M.; Tsivion, D.; Mahalu, D.; Raslin, O.; Joselevich, E. Self-Integration of Nanowires into Circuits Via Guided Growth. *Proc. Natl. Acad. Sci. U.S.A.* **2013**, *110*, 15195−15200.
(21) Fortuna, S. A.; Wen, J. G.; Chun, I. S.; Li, X. L. Planar GaAs Nanowires on GaAs (100) Substrates: Self-Aligned, Nearly Twin-Defect Free, and Transfer-Printable. *Nano Lett.* **2008**, *8*, 4421−4427.
(22) Nikoobakht, B.; Michaels, C. A.; Stranick, S. J.; Vaudin, M. D. Horizontal Growth and in Situ Assembly of Oriented Zinc Oxide Nanowires. *Appl. Phys. Lett.* **2004**, *85*, 3244−3246.
(23) Nikoobakht, B.; Herzing, A. Formation of Planar Arrays of One-Dimensional P−N Heterojunctions Using Surface-Directed Growth of Nanowires and Nanowalls. *ACS Nano* **2010**, *4*, 5877−5886.
(24) Jaszek, R. Carrier Scattering by Dislocations in Semiconductors. *J. Mater. Sci. Mater. Electron.* **2001**, *12*, 1−9.
(25) Hÿtch, M.; Snoeck, E.; Kilaas, R. Quantitative Measurement of Displacement and Strain Fields from Hrem Micrographs. *Ultramicroscopy* **1998**, *74*, 131−146.
(26) Geis, M. W.; Flanders, D. C.; Smith, H. I. Crystallographic Orientation of Silicon on an Amorpous Substrate Using an Artificial Surface-Relief Grating and Laser Crystallization. *Appl. Phys. Lett.* **1979**, *35*, 71−74.
(27) Ismach, A.; Kantorovich, D.; Joselevich, E. Carbon Nanotube Graphoepitaxy: Highly Oriented Growth by Faceted Nanosteps. *J. Am. Chem. Soc.* **2005**, *127*, 11554−11555.
(28) Ismach, A.; Joselevich, E. Orthogonal Self-Assembly of Carbon Nanotube Crossbar Architectures by Simultaneous Graphoepitaxy and Field-Directed Growth. *Nano Lett.* **2006**, *6*, 1706−1710.
(29) Bonafede, S. J.; Ward, M. D. Selective Nucleation and Growth of an Organic Polymorph by Ledge-Directed Epitaxy on a Molecular Crystal Substrate. *J. Am. Chem. Soc.* **1995**, *117*, 7853−7861.
(30) Joselevich, E. Self-Organized Growth of Complex Nanotube Patterns on Crystal Surfaces. *Nano Res.* **2009**, *2*, 743−754.
(31) Ismach, A.; Segev, L.; Wachtel, E.; Joselevich, E. Atomic-Step-Templated Formation of Single Wall Carbon Nanotube Patterns. *Angew. Chem., Int. Ed.* **2004**, *43*, 6140−6143.
(32) Fischer, A.; Kühne, H.; Richter, H. New Approach in Equilibrium Theory for Strained Layer Relaxation. *Phys. Rev. Lett.* **1994**, *73*, 2712−2715.
(33) Ertekin, E.; Greaney, P. A.; Chrzan, D.; Sands, T. D. Equilibrium Limits of Coherency in Strained Nanowire Heterostructures. *J. Appl. Phys.* **2005**, *97*, 114325−114325-10.
(34) Chin, A. H.; Ahn, T. S.; Li, H.; Vaddiraju, S.; Bardeen, C. J.; Ning, C.-Z.; Sunkara, M. K. Photoluminescence of GaN Nanowires of Different Crystallographic Orientations. *Nano Lett.* **2007**, *7*, 626−631.
(35) Nikoobakht, B.; Eustis, S.; Herzing, A. Strain-Driven Growth of Zinc Oxide Nanowires on Sapphire: Transition from Horizontal to Standing Growth. *J. Phys. Chem. C* **2009**, *113*, 7031−7037.

Guided Growth of Epitaxially Coherent GaN Nanowires on SiC

*David Tsivion and Ernesto Joselevich**

Department of Materials and Interfaces, Weizmann Institute of Science, Rehovot 76100, Israel.

Supporting Information

1. Materials and methods.
2. SEM and image of the Pd catalyst prior to the NW growth (Figure S1).
3. Additional SEM images of NW (Figure S2-S4)

1. Materials and methods

Substrate preparation

We used three Si-terminated face of three different SiC substrates (Xiamen Powerway Advanced Material): (0001) plane of 6H-SiC and 4H-SiC, and a vicinal (0001) plane of 4H-SiC tilted by 4° toward $[11\bar{2}0]$. Prior to use, the substrates were sonicated for 10 minutes in acetone, then rinsed in acetone, isopropyl alcohol (IPA), and deionized H_2O, then blow-dried in N_2. After that, the oxide layer was removed by 1:6 buffered oxide etch, and the substrates were rinsed again in deionized water and blow-dried in N_2.

Catalyst deposition and patterning

The Pd catalyst was usually deposited by electron-beam evaporation of a thin (2-6Å) metal layer (Fig. S1). First, the areas for catalyst deposition were defined using standard photolithography with negative or positive photoresists. After pattern development and brief surface cleaning by oxygen plasma (March Plasmod GCM 200, 2 min, 1 sccm of O_2, 100 W) thin films (2-6 Å) of Pd were deposited by electron-beam evaporation, followed by liftoff in acetone. When heated to the temperature of the NW growth process, these rough Pd films create nanoparticles that serve as catalyst for the VLS growth of nanowires. The Pd nanoparticles probably undergo some degree of Ostwald ripening in the time between moving the furnace over the sample and the actual beginning of NW growth. In addition, Pd nanoparticles were created by drop-casting a solution of bis(dibenzylideneacetone)palladium in 1,2-dichloroethane without any further treatment and yielded similar results.

Nanowire synthesis

Nanowire growth was carried out in a quartz tube inside a tube furnace with fast heating capabilities (25°C to 1000°C in 5 minutes). The Ga atoms were supplied from Ga_2O_3 held at

950-1000 °C, while the samples were held downstream at a temperature of 950°. N atoms were supplied from NH_3 (99.999%) at a flow of 3 sccm. H_2 was used as carrier gases (99.999%, Gordon Gas, further filtered to reduce O_2 and H_2O levels) at a flow of 60-90 sccm. In a typical experiment, a substrate with catalyst was placed on a fused-silica carrier plate and inserted to a 25 mm diameter quartz tube. The tube was inserted into a split oven and purged of oxygen by 5 cycles of pumping to 3 mbar and purging with N_2 at elevated temperature. Once the tube was purged, N_2 was streamed into the tube, and pressure was maintained at 400 mbar. Once the desired temperature (1000 °C) is achieved, the oven was moved over the Ga_2O_3 powder, and turned off at the end of the growth time (usually 5-30 minutes).

Microscopic characterization

The grown nanowires were imaged using field-emission SEM (Supra 55VP FEG LEO Zeiss) at low working voltages (1-5 kV). Atomic force microscopy (AFM, Veeco, Multimode Nanoscope IV) images were acquired in air tapping mode. Thin lamellae for TEM characterization were made using a FEI Helios DualBeam microscope, and inspected using a FEI Tecnai F30-UT field emission TEM, equipped with a parallel EELS (Gatan imaging filter) operating at 300 kV. TEM digital images were recorded using a Gatan Ultrascan1000 CCD camera. TEM images were analyzed to determine crystallographic orientation and epitaxial relations using Fourier transform (FFT) from selected areas in the nanowire cross-sections. Indexing of the FFT peaks was done according to crystallographic tables for bulk GaN.

Optical characterization

Photoluminescence spectra from single GaN nanowires were acquired with a Jobin-Yvon LabRam HR 800 micro-Raman system, equipped with a liquid-N_2-cooled detector. For the excitation, we used a He-Cd laser at 325 nm. The laser power on the sample was 5 mW. The

measurements were taken with a 2400 g mm^{-1} grating for the UV (spectral resolution 4 cm^{-1}) and a confocal microscope with a 100 μm aperture and a 10 μm laser spot.

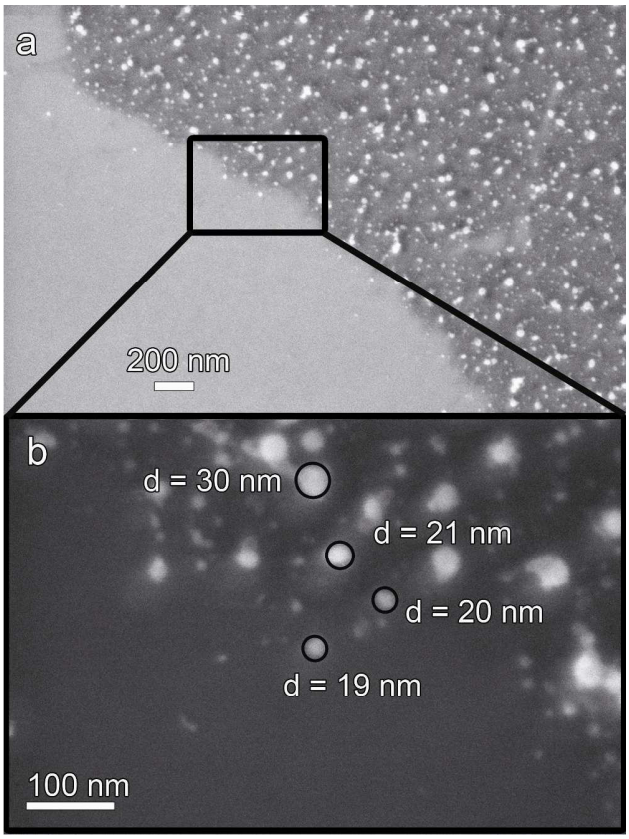

Figure S1. Patterned Pd catalyst. The evaporated Pd layer was nominally 4 Å in thickness and underwent dewetting at 550 °C for 5 minutes in a reducing atmosphere. (a) Low magnification SEM image. (b) Higher magnification image of the area indicated in (a).

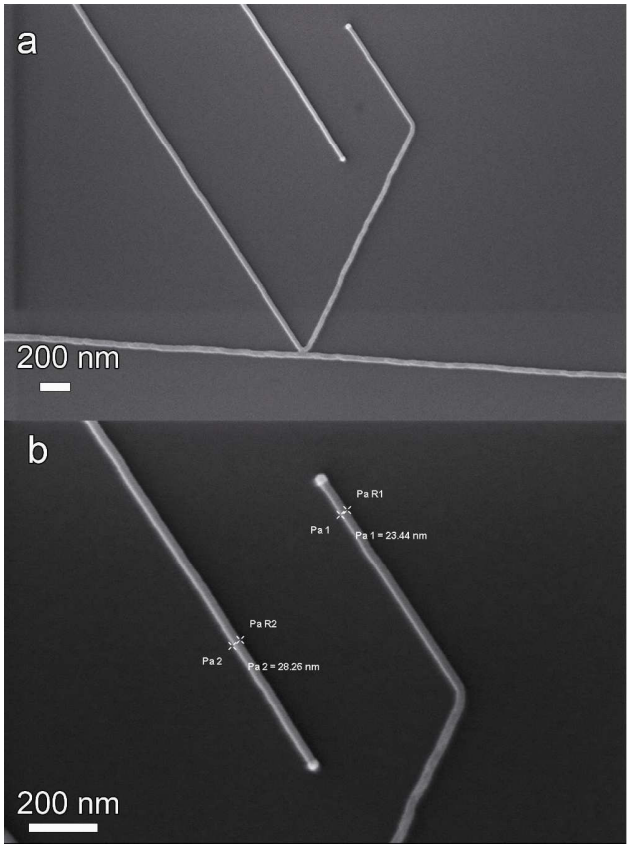

Figure S2. Horizontal GaN NW on Flat (0001) SiC. (a) Low magnification SEM image. (b) Higher magnification image of (a). The catalyst nanoparticle is clearly visible at the end on the two NWs.

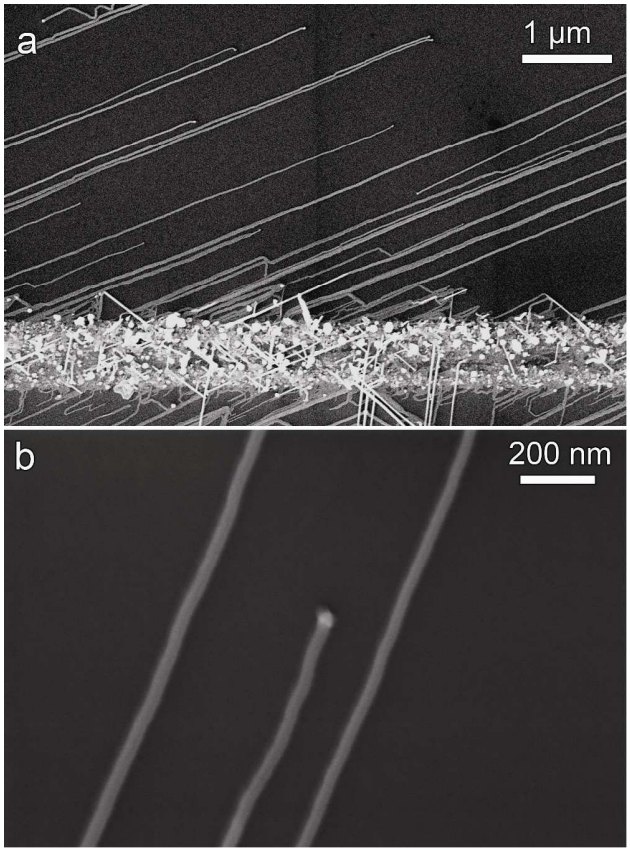

Figure S3. Two images of horizontal GaN NW on vicinal (0001) plane of 4H-SiC tilted by 4° toward $[11\bar{2}0]$. The Pd catalyst pattern is the thick, white stripe. The NWs can be clearly seen growing into the clean substrate on the two sides of the catalyst pattern.